



HAL
open science

FRACTAL ANALYSIS OF LIQUID ATOMIZATION PROCESSES. PART 1: METHODOLOGY

Sébastien Grout, Jean Cousin, Christophe Dumouchel

► **To cite this version:**

Sébastien Grout, Jean Cousin, Christophe Dumouchel. FRACTAL ANALYSIS OF LIQUID ATOMIZATION PROCESSES. PART 1: METHODOLOGY. ICLASS 2006, Aug 2006, Kyoto (Japan), Japan. <hal-03994313>

HAL Id: hal-03994313

<https://normandie-univ.hal.science/hal-03994313v1>

Submitted on 17 Feb 2023

HAL is a multi-disciplinary open access archive for the deposit and dissemination of scientific research documents, whether they are published or not. The documents may come from teaching and research institutions in France or abroad, or from public or private research centers.

L'archive ouverte pluridisciplinaire HAL, est destinée au dépôt et à la diffusion de documents scientifiques de niveau recherche, publiés ou non, émanant des établissements d'enseignement et de recherche français ou étrangers, des laboratoires publics ou privés.



HAL Authorization

Paper ID ICLASS06-050

FRACTAL ANALYSIS OF LIQUID ATOMIZATION PROCESSES. PART 1: METHODOLOGY

Sébastien Grout, Dr. Jean Cousin, Dr. Christophe Dumouchel

CNRS UMR 6614 – CORIA, Université et INSA de Rouen
76801 Saint Etienne du Rouvray, France
email: *name@coria.fr*

ABSTRACT This work, presented in two parts, investigates the relevance of using fractal analysis to characterize and study liquid flow atomization processes and participates to the required effort of conducting experimental investigations on primary break-up processes. This first part tackles the problem of the method. Several methods to determine fractal dimension are available but none of them is a priori better than any other and they all require to be tested. Three methods are tested on synthetic images that have similar characteristic features as the liquid flow images we intend to analyze. The results show that Euclidean Distance Mapping (EDM) method is the most appropriate in our case where local fractal dimension wants to be determined. It is shown that this method is well adapted to determine both the textural and the structural fractal dimensions of an object. These two fractal dimensions characterize the tortuosity of the object boundary and the tortuosity of the object itself, respectively. It is also found that EDM allows building fractal dimension distribution which is useful to qualify the fractalness of the analyzed object.

Keywords: Primary liquid atomization process, fractal analysis

1. INTRODUCTION

A rapid overview of the works available in the literature shows that the question of liquid flow distortion – prior step to any liquid atomization process – has been widely investigated from a theoretical point of view but that experimental investigations on primary break-up processes are lacking. Primary break-up designates the process of liquid detachment from the continuous liquid flow connected to the nozzle. Chigier [1] pointed out that the primary break-up region of an atomizing liquid flow requires to be investigated since it is the vital link between the liquid emerging from the nozzle and the fully developed spray. Furthermore, he added that imaging remains the sole technique for obtaining information about liquid sheets and jets emerging from nozzles and their subsequent break-up and that efforts must be made to record, analyze and interpret the break-up process. The work reported in this study intends to participate to this effort.

Illustrations of atomizing liquid flows presented and discussed in [2] show that whatever the working conditions, an atomizing liquid flow is a geometric object with complex boundaries and that drop and ligament detachment is a function of the shape of the stream. Therefore, it appears relevant to characterize the shape of the liquid flow during atomization. This study, that is presented in two parts, investigates the possibility of using the fractal dimension concept to characterize atomizing liquid flows.

The fractal dimension is an extension of the Euclidean dimension and allows describing complex boundaries. For a straight line, Euclidean and fractal dimensions are equal to 1. For a line inscribed in a plane, the fractal dimension varies from 1 if the line is straight to 2 if the line is so tortuous that it fully covers the whole plane. Fractal dimension is a measure of the tortuosity, fragmentation or roughness of a surface or a line that is strictly or statistically self-similar over a range of scales, i.e., pieces of the pattern,

when magnified, resemble to the whole [3].

Fractal analysis is used in several fields to characterize object with complex shapes. In medicine, it characterizes neuron and cell morphology [3-5]. In physics, fractal analysis has been widely applied to characterize scalar interface in turbulent flows [6]. In combustion, the morphology of front flame [7] and of soot particles [8] can be related to a fractal dimension.

The use of fractal analysis in liquid atomization and spray systems has received very little attention so far. Chehroudi and Talley [9] used a fractal analysis to characterize the envelop of dense sprays as a function of the atmospheric conditions. As far as the characterization of liquid flow primary atomization region is concerned, only two approaches are available. The first one is due to Shavit and Chigier [10] who considered the liquid gas interface of an air assisted cylindrical liquid jet. They succeeded in determining a fractal dimension of the liquid gas interface and found that, as going downstream from the nozzle exit, this fractal dimension increased, reached a maximum and decreased. The region where the fractal dimension is maximum was identified as the region where the liquid break-up is the more effective. Furthermore, the maximum fractal dimension reported a relationship with some mean diameter of the spray drop size distribution. A similar approach was followed in a previous study [11] in a totally different situation. The liquid atomization process was not controlled by a gaseous turbulent assisting flow but by the turbulence generated in the liquid flow itself. The conclusions of that work confirmed the general trend reported by Shavit and Chigier [10]. Although these two investigations showed the relevance of using fractal analysis to liquid atomization process, several points remained unanswered among which, what is the best method to determine liquid interface fractal dimension? What is the quality of the atomization process fractalness? What kind of physical information can be deduced from a

fractal analysis? This last question is important.

A fractal analysis may bring other information than the sole fractal dimension. In the literature, fractal objects are divided in two groups: linear (or ideal) fractals and non-linear (or natural) fractals (Foroutan-pour et al. [12]). Linear (or ideal) fractals result from an absolute generating process. For these objects the fractal dimension is analytical and can be exactly calculated over a semi infinite domain. Non-linear (or natural) fractals result from a statistical generating process. Physical objects fall into this category and are fractal in a range of physical cutoff length scales. The knowledge of these length scales might be interesting but requires an appropriate technique to determine the fractal dimension. The question of the fractal analyzing method is addressed in the present article.

There are several techniques to determine the fractal dimension of 2D contours. Smith et al. [5] classified them in two categories; the Length methods and the Mass method. Length methods are extensively used. They can be subdivided into the Box Counting methods and the Sausage methods. The previous attempts of atomization process fractal analyses were performed with a Box Counting method [10, 11]. The Mass Methods are less used. We can find applications of this method in Panico and Sterling [3], Caserta et al. [4] and in Smith et al. [5]. These fractal methods have been compared in several working conditions [3, 5, 7, 9, 12]. According to these works (and others) it appears impossible to know whether one technique is better than any other in a given situation. It seems therefore reasonable to test several methods on images of mathematical (linear) fractals paying attention that these images are of the same type as those of the physical behavior we want to characterize. This work is presented in this article.

Three fractal dimension determination methods are tested on synthetic images. These images, presented in the next section, have similar characteristic features as the liquid flow images we want to analyze and contained 2D mathematical contour of known fractal dimension. As far as the fractal dimension methods are concerned, it is decided to use a Box Counting method, a Sausage method and a Mass Method. These techniques are presented in section 3 of this article and the application of these methods to analyze the synthetic images is presented and discussed in section 4.

2. DESCRIPTION OF THE IMAGES

The atomizing liquid flows that will be analyzed are produced by a simplified compound (or cavity) nozzle. Compound injectors, widely used in low pressure gasoline injection, are made of a superposition of two or three disks. The internal nozzle geometry imposes drastic deflections to the flow and favors the development of complex issuing flow structures. At the exit section, the flow shows a double swirl and a consistent turbulent level. It was shown in a previous investigation (Dumouchel et al. [14]) that the aerodynamic forces have no effect on the atomization process because of low injection pressures. The atomization efficiency is related to the kinetic energy of the non axial flow component as well as to the turbulent kinetic energy at the nozzle exit, both characteristic features being functions of the injection pressure and of the nozzle geometry. The

simplified cavity nozzle used in the present investigation is described in the second part of this study.

An example of the liquid flow issuing from this nozzle is shown in Fig. 1-a. This image was obtained with heptane and an injection pressure of 0.2 MPa. Thanks to the use of appropriate camera and light source, the image shows good spatial and temporal resolutions. The fractal analysis we intend to perform concerns the continuous liquid flow only and detached droplets and ligaments are not taken into account and are removed from the image. Thus, the objects to be analyzed are contours of the continuous issuing flow as illustrated in Fig. 1-b. (Details on the experimental set-up, diagnostics and on the image analyzing technique are given in the second part of this study).

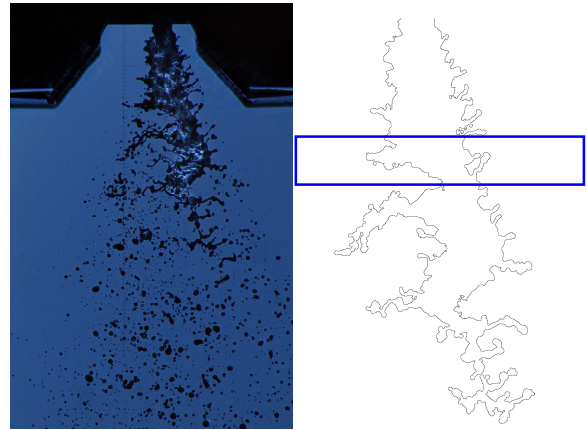


Figure 1: Left – Example of liquid flow issuing from the simplified compound nozzle ($\Delta P_i = 0.2$ MPa, fluid: Heptane), Right – Associated contour of the continuous liquid stream. The rectangle shows the Analyzing Window delimiting portion of the flow for the determination of local fractal dimension (not on scale)

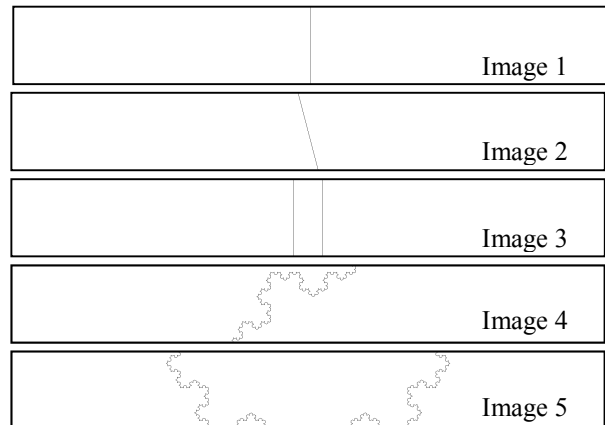


Figure 2: Synthetic images

Following previous studies (Shavit and Chigier [10], Dumouchel et al. [11]), we are interested in the determination of the local fractal dimension in order to investigate its evolution from the nozzle exit to the end of the primary atomization process. To achieve this, the fractal dimension is determined on portions of the liquid flow

delimited by an analyzing window (see Fig. 1-b). This window is 257 pixels height and is as wide as the initial image, i.e., 2,016 pixels. Thus, the objects to be analyzed are two contour parts, more or less close according to the distance from the nozzle. They are different than most of the objects analyzed in the literature that are closed contours. This justifies the present study which consists in testing fractal analysis methods on synthetic images of mathematical objects with a known fractal dimension.

The synthetic images were designed to reproduce the characteristic features of the atomizing liquid flow images. They have the same size as the analyzing window (257x2,016 pixel²) and contain one or two portion(s) of objects. Five images are analyzed, they are presented in Fig. 2.

Image 1 is a single vertical straight line positioned in the middle of the image. The fractal dimension of this object is 1. Image 2 is an inclined single straight line (the inclination angle is equal to 15°). Although this image is similar to the previous one since the objects they contained have the same fractal dimension, the line in Image 2 will allow quantifying image digitalization effect. Image 3 contains two parallel straight lines. The distance between the two lines is 100 pixels. The analysis of this image will illustrate the influence of the presence of two contour portions on the determination of the fractal dimension. Image 4 contains a portion of a 5-order triadic Koch coast line. The Koch line is a linear (or ideal) fractal often used in the literature to test fractal methods. It results from an absolute generating process with a known construction rule. Its fractal dimension is analytical and equal to 1.2618. The portion of Koch coast line in Image 4 is inclined. Finally, Image 5 contains two portions of 5-order triadic Koch coast line.

3. DESCRIPTION OF THE FRACTAL ANALYZING METHODS

The fractal analysis of the synthetic images presented above is conducted with three methods: the Minimum Grid Counting method, the Euclidean Distance Mapping method and the Mass Method.

3.1. Minimum Grid Counting method (MGC)

The MGC method is a length method that derives from the Box Counting Method. It consists in superimposing a regular grid of square elements of size r on the image and in counting the number $N(r)$ of squares intersecting the contour. Plotting $N(r)$ as a function of r on a logarithm scale reports a linear behavior if the contour is fractal. This log-log plot is called the Richardson-Mandelbrot plot. The fractal dimension of the object can be deduced from the slope of this plot: the Box Counting Method connects the number $N(r)$ and the spatial scale r by the relation:

$$N(r) = Kr^{-\delta} \quad (1)$$

where K is a constant and δ is the fractal dimension of the object. This technique was used by Shavit and Chigier [10]. It was noted in the literature (Panico and Sterling [3], Foroutan-pour et al. [12], Dumouchel et al. [11]) that the number $N(r)$ is sensitive to the position of the grid upon the

object. Panico and Sterling [3] and Dumouchel et al. [11] averaged the number $N(r)$ on all possible grid positions, whereas Foroutan-pour et al. [12] noted that the strict estimation of a fractal dimension value requires the minimum box covering. These two approaches are not equivalent. For $r = 1$, a single grid position exists and both approaches report the same number $N(r)$. However, for large spatial scales (large r), the number $N(r)$ averaged on the grid position is always greater than the minimum number $N(r)$. Thus, according to Eq. (1), the average counting reports smaller fractal dimensions than the minimum counting. This might explain why, using the average counting, Triballier [15] reported fractal dimension less than 1 for contour lines barely tortuous. To avoid such non-physical results, it was decided to use the minimum $N(r)$ for each value of r and to refer to this approach as the Minimum Grid Counting method.

3.2. Euclidean Distance Mapping method (EDM)

Classified in the Sausage Methods, the EDM method is also a length method. Each pixel of the image is attributed a gray level that is equal to the shortest distance, expressed in pixel, between this pixel and the contour: if the distance is r , the gray level attributed to this pixel is r also. Then, for each value of r , the number $N(r)$ of pixels with a brightness less or equal to r are counted. This number of pixels coincides with the area of a ribbon around the contour, each external pixel of the ribbon being at an equal distance from the contour. There are several ways of calculating the fractal dimension. According to Bérubé and Jébrak [13], the more practical is to plot the number $N(r)$ against the width of the corresponding ribbon, i.e., $2r+1$. This Richardson-Mandelbrot plot is linear if the object is fractal and the fractal dimension δ can be obtained from the slope of the line by using the relationship:

$$N(r) = K(2r+1)^{2-\delta} \quad (2)$$

where K is a constant. This method was found more reliable than box methods to determine the fractal dimension (Hall et al. [7], Bérubé and Jébrak [13]). Furthermore, EDM is more isotropic, more efficient and generally more precise (Chehroudi and Talley [9]).

3.3. Mass Method (MM)

The third method to be tested is called the Mass Method or the Sandbox method (Panico and Sterling [3], Smith et al. [5]). This method is a variant of the box-counting method [4]. A pixel belonging to the contour is chosen as a centering site. In the present approach, square boxes of size r are centered on it and, for each value of r , the total number $N(r)$ of black pixels falling within the square is counted. The Richardson-Mandelbrot plot shows the number $N(r)$ as a function of r in a logarithm scale. A fractal object reports a linear Richardson-Mandelbrot plot and the fractal dimension δ is obtained from the relationship:

$$N(r) = Kr^{\delta} \quad (3)$$

where K is a constant. For a given object, the procedure must be repeated using as centered sites all contour pixels

belonging to a region delimited by the radius of gyration of the object (Panico and Sterling [3], Smith et al. [5]). The fractal dimension of the object is the average of the fractal dimensions obtained with all the centering sites.

The MM provides more information about the fractal object than the length method. It deals with a quantitative description of the contour and also leads to the concept of lacunarity and multifractals (Smith et al. [5]).

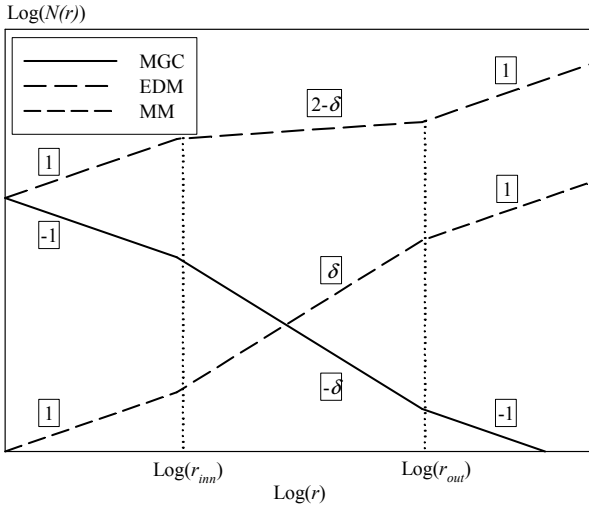


Figure 3: Theoretical Richardson-Mandelbrot plots according to the method (Case of a natural fractal: the object is fractal in the scale range delimited by r_{inn} and r_{out} . Quantity in squares indicate local slope)

The three methods described above and tested in the present work report different Richardson-Mandelbrot plots that are compared in Fig. 3 for a natural fractal with a self-similarity spanning in the length scale interval $[r_{inn}; r_{out}]$. Within the range of these scales, the slope of the Richardson-Mandelbrot plot is a function of the fractal dimension and of the method used (see Eq. (1)-(3)). Thus, the determination of the fractal dimension requires the identification of the linear regions in the Richardson-Mandelbrot plot, which is, most of the time, a tricky task. In the present work, the local slope graph technique introduced by Panico and Sterling [3] is used. It consists in calculating linear regressions over a window containing a limited number of consecutive points in the log-log plot and to investigate the evolution of the local slope as the window slides over the entire r -range. For a fractal object, this technique reports a local slope constant over a range of length scales. If no region with constant local slope is found, the object is not fractal. In the present study, local linear regression are performed over seven consecutive points in the Richardson-Mandelbrot plot. As noted by Panico and Sterling [3] we observed that smaller intervals for local slope calculation increased the noise but did not affect the apparent linearity in Richardson-Mandelbrot plots.

4. RESULTS

The three methods described above are tested with the

synthetic images (Fig. 2). For the MGC method, the size r of the square elements varies from 1 to 257 pixels, and the EDM method is applied with an interval of brightness level r ranging from 1 to 126 pixels. As explained above, the MM method is local and requires defining contour pixels as centering sites. It is important that the size r of the structuring element varies in the same interval for each pixel centering site. To satisfy this requirement, the centering sites are the pixels of the contour intercepting the middle line of the analyzing window and the square size varies from 1 to 257 pixels, taking only the odd values to make sure that the centering sites is always the middle point of the square. The symmetry of Images 1, 2 and 3 renders unnecessary an statistical approach and the three methods are applied on a single image each time. However, they are applied on 150 images for Images 4 and 5, each image showing a different part of the Koch coast line but equivalent in size. The Richardson-Mandelbrot graphs are plotted with the average of the numbers $N(r)$ obtained for each image.

The result of the analysis of Image 1 is given in Fig. 4. This figure compares the local slope graph obtained with the three methods. In order to facilitate the comparison between the three methods the local slope graph shows the value of δ calculated from Eq. (1) to (3) according to the method. Furthermore, the results presented in this paper are smoothed by performing sliding average of δ on 15 consecutive values of r , for each value of r . It is interesting to add that this smoothing precaution reported a minor influence on the initial results.

Figure 4 shows that, over the whole length scale range, both the EDM and MM methods report a constant local slope equal to the expected value of 1. However, it can be seen that the MGC method is not convenient at all for this kind of image. This behavior is due to the fact that the range of scale r used for the MGC method is not appropriate to the size of the image. It is recommended in the literature (Foroutan-pour et al. [12]) that the maximum box size in box counting methods must not exceed 25% of the smallest size of the image. If not, very poor information is returned by the method. This requirement in our case limits the value of the maximum square size to 64 pixels. According to Fig. 4 this limit appears too high as the fractal dimension of the line is correctly calculated by the MBC method for a spatial scale r ranging from 1 to 30 pixels only. The results obtained for the other images confirm the poor appropriateness of the MGC method for the kind of images analyzed here. Thus, in the following, the results obtained with the EDM and MM methods are presented and discussed only.

Figure 5 presents the local slope obtained for the analysis of an inclined straight line (Image 2). This figure shows that the MM method is not at all affected by the digitalization of the object. However, the digitalization slightly affects the EDM efficiency. This is mainly observable at small spatial scales where digitalization is interpreted as tortuosity. Thus, the fractal dimension is overestimated in this region. However, the EDM method reports a very acceptable value of the fractal dimension when the spatial scale varies from a minimum scale equal to 50 pixels to 250 pixels. Thus, to minimize the influence of the image digitalization for the EDM method, the spatial scale should not be smaller than 50 pixels.

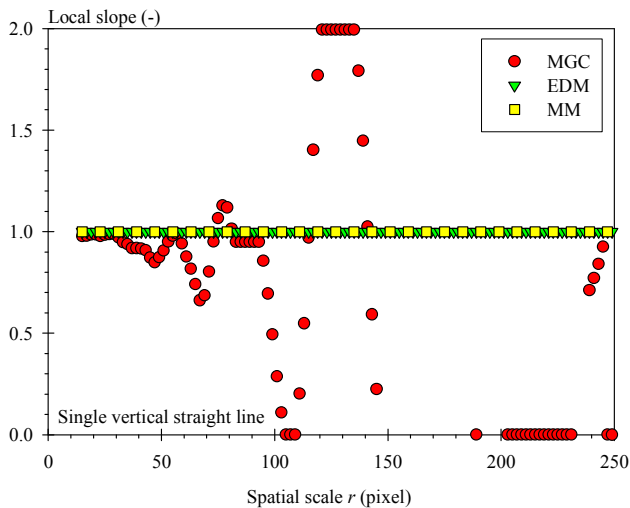


Figure 4: Local slope graphs obtained for Image 1. Comparison between the three methods.

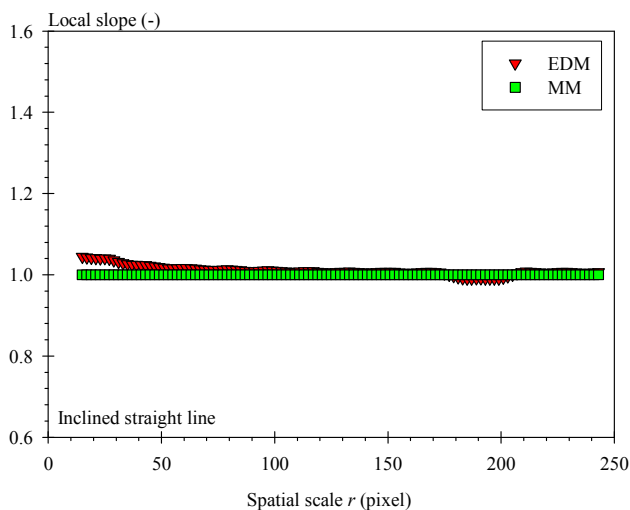


Figure 5: Local slope graphs obtained for Image 2. Comparison between EDM and MM methods.

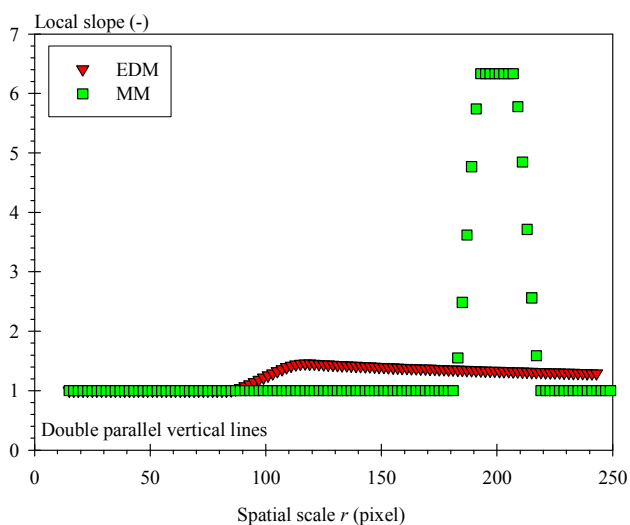


Figure 6: Local slope graphs obtained for Image 3. Comparison between EDM and MM methods.

The results obtained for Image 3 are shown in Fig. 6. The test conducted with this image shows the influence of the presence of two portions of the same contour in the image. For both methods, the presence of two contour portions has a similar effect, which is an increase of the local slope at a given spatial scale that depends on the method. When the image is analyzed at small scales (small value of r), both lines are analyzed independently and both methods report a fractal dimension equal to 1. However, for a given spatial scale r , a sudden change in the number $N(r)$ is observed. This change, which is due to the fact that the two line portions are seen as a single object at this scale, induces an increase of the local slope. For the EDM method, this increase is observed for a spatial scale of the order of 100 pixels (see Fig. 6). This value, which is equal to the distance between the two lines, is obtained because there is no pixel farther than 50 pixels from the nearest contour between the two lines, keeping in mind that the spatial scale shown in Fig. 6 is twice the nearest distance from the contour (see Eq. (2)). For the MM method, the number of contour pixels intersecting the square centered on one line is suddenly doubled when the square hits the second line, that is, when its size is 200 pixels as found in Fig. 6. However, for larger spatial scale, this number of pixels retrieves a linear dependence with the square size and the local slope returns to the value of the line fractal dimension. The width and height of the local slope peak reported by the MM approach in Fig. 6 are determined by the point interval used for the local slope calculation and by the smoothing filter and are not physically relevant. From this point of view, the results obtained with the EDM method are different: for large spatial scales, the method reports an almost constant local slope, suggesting the existence of a fractal dimension greater than 1 within the large scale range.

Bérubé and Jébrak [13] pointed out the influence of the overall structure on the fractal dimension. They showed that objects with similar boundaries reported greater fractal dimension if they were elongated, and that the EDM method was particularly sensitive to this aspect. This is interesting and illustrates the difference between the textural and the structural fractal dimensions introduced by Kaye [8]. The textural fractal dimension of an object characterizes the tortuosity of the boundary of the object, whereas the structural fractal dimension characterizes the tortuosity of the whole object. In atomization, this difference is interesting to make since it dissociates the tortuosity that characterizes the formation of ligaments (structural fractal dimension) with the one characterizing the drop formed from interface peeling off (textural fractal dimension). Thus, the increase of the EDM local slope in Fig. 6 characterizes the structure of the object made of two parallel line portions. This object has a certain spatial covering capacity which explains the existence of a fractal dimension. The slight decrease of the local slope at large spatial scales is due to the lack of self similarity of the structure of the object. Finally, it is interesting to note that the scale at which the EDM local slope changes corresponds to the limit between textural length scales and structural length scales.

The results obtained for a single five-order Koch line are presented in Fig. 7. As explained above, in this case as

well as for image 5, the Richardson-Mandelbrot plots and local slope graphs result from the analysis of 150 images. The theoretical fractal dimension of the triadic Koch coast line is also shown in Fig. 7 ($\delta=1.2618$). This figure shows the good behavior of the EDM method that reports a pretty constant local slope for a spatial scale ranging from 25 pixels to 250 pixels. It can be also observed that the unfavorable influence of the image digitalization is not as pronounced as it was for Image 2 (see Fig. 5). The result of the analysis of Image 4 with the MM method is more problematic. Although the mean local slope averaged over the whole range of spatial scales is close to the theoretical fractal dimension, there is no spatial scale interval over which the local slope is constant. According to the definition of a fractal object, the MM method induces the idea that the contour in Fig. 7 is not fractal, which is incorrect. Thus, it appears that for the type of images studied in the present work, the MM method is not efficient to dissociate fractal objects with non fractal ones.

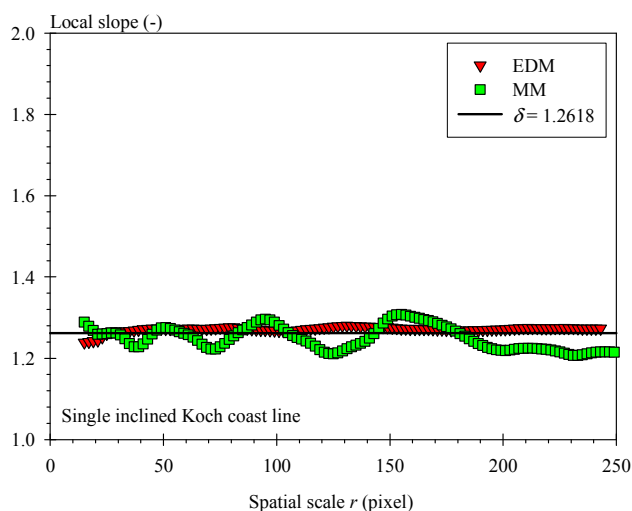


Figure 7: Local slope graphs for Image 4. Comparison between the EDM and the MM methods.

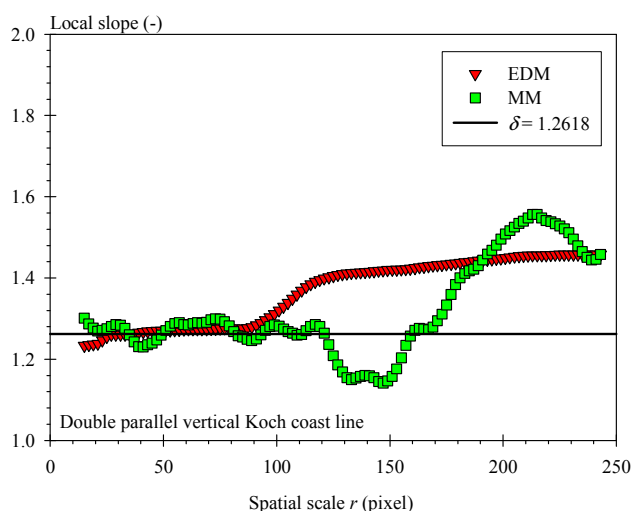


Figure 8: Local slope graphs for Image 5. Comparison between the EDM and the MM methods.

The results obtained for Image 5 (Double Koch coast line) and shown in Fig. 8 lead to a similar conclusion. When analyzing the object at small spatial scales, the EDM method reports a constant local slope equal to the expected value of the Koch line fractal dimension. As for Image 3 (Fig. 6), at small spatial scale, each Koch line is analyzed independently. For a spatial scale of the order of 100 pixels, the EDM method reports a sudden increase of the local slope. The value 100 pixels being the shortest distance between the two Koch lines, it also corresponds to the spatial scale at which the two lines start to be seen and analyzed as a single object. When the spatial scale continues increasing, the EDM method shows a local slope that evolves towards a constant value of 1.47. Thus, the analysis conducted with the EDM method says that the double Koch lines separated by 100 pixels has a textural fractal dimension equal to 1.26 and a structural dimension equal to 1.47.

As for the analysis of Image 4, the application of the MM method to analyze Image 5 reports an unexploitable local slope graph. Once again, there is no clear spatial scale interval over which the local slope is constant. This result should lead to the conclusion that the object in Image 5 is not fractal.

According to the tests presented just above, it appears that the EDM method is appropriate to determine both textural and structural fractal dimensions whereas the MM method allows determining the textural fractal dimension only (see Fig. 6 for instance). However, as noticed in Fig. 7, the MM method fails in deriving the fractal dimension of a Koch line. To explain this, one has to keep in mind that these two methods analyze the contour differently. For each image, the EDM method analyzes the all contour in the image at the same time whereas the MM method performs a local analysis by using a limited number of centering sites for each image. Indeed, only contour pixels intercepting the pixel middle line of the image are used as centering sites. Thus, to have a result statistically representative, the MM method must be conducted on several images and the number of images used likely influences the quality of the result. To check this, the influence of the number of images on the MM method was investigated. For comparison, the same test is performed with the EDM method. This test consists in applying both methods on several sets of Image 4 (the single Koch coast-line). Figure 9 shows the local slope graphs obtained with the MM method and for several numbers of analyzed images. To make the results more easily readable, symbols have been replaced by lines. For comparison, the expected theoretical value $\delta=1.2618$ is also indicated in this figure. The results presented in Fig. 9 show that the number of images considerably influences the local slope graph obtained with the MM method. When a single image is analyzed, the local slope oscillates around the theoretical value and the amplitude of this oscillation is rather high. When the number of images increases, the amplitude of the oscillation decreases. However, this test shows that a minimum number of a few thousands of images are necessary to have a reliable results with the MM method. In the previous application of this method, (Figs. 7 and 8), the number of images analyzed was 150 only which, according to the results shown in Fig. 9, is far not enough. This explains the poor quality of the results obtained with the MM method when analyzing Images 4 and 5 (Figs. 7

and 8).

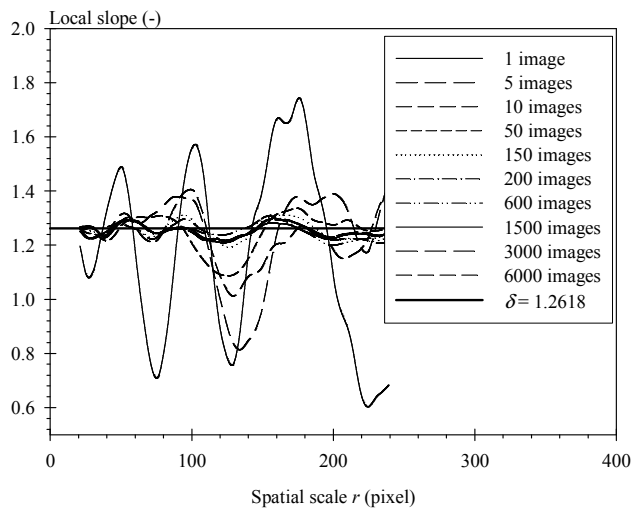


Figure 9: Influence of the number of images on the local slope graph (MM method, Image 4).

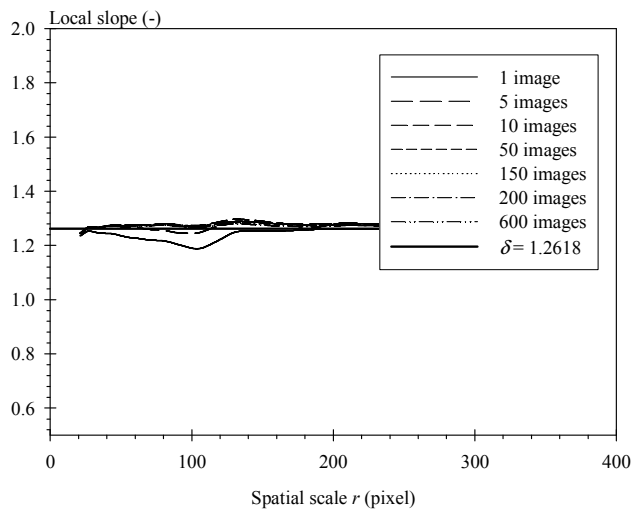


Figure 10: Influence of the number of images on the local slope graph (EDM method, Image 4).

For comparison Fig. 10 presents a similar test performed with the EDM methods. The result is totally different. Indeed, it can be seen that the number of images has a reduced influence on the local slope graph obtained with the EDM method. An interesting point to be noticed is that, even when analyzing a single image, the EDM method reports a non negligible spatial scale interval over which the local slope is constant and equal to the theoretical value. This interval is positioned in the large spatial scales. For small spatial scales, we might suspect that the EDM analysis is affected by the image digitalization because a Koch line is a succession of straight lines whose representation is more or less deformed by digitalization according to their direction.

These last results are important. First, it appears that the MM method is a reliable method to determine the

fractal dimension of portion of liquid flow provided that a large number (a few thousands) of images are analyzed. Such an approach would be very time consuming and is not adopted here. Second, it appears that the application of the EDM method on a single image is possible. This allows us performing the fractal analysis in a different way. By analyzing each image independently, one will be able to plot a fractal dimension distribution from the analysis of a high number of images. According to Smith et al. [5], this distribution will qualify the fractalness of the physical process investigated (here, the atomization process). A distribution with a stiff peak indicates that each image reports the same fractal dimension and that the process is fractal. Otherwise, that is if the fractal dimension distribution is large, the process investigated is multifractal.

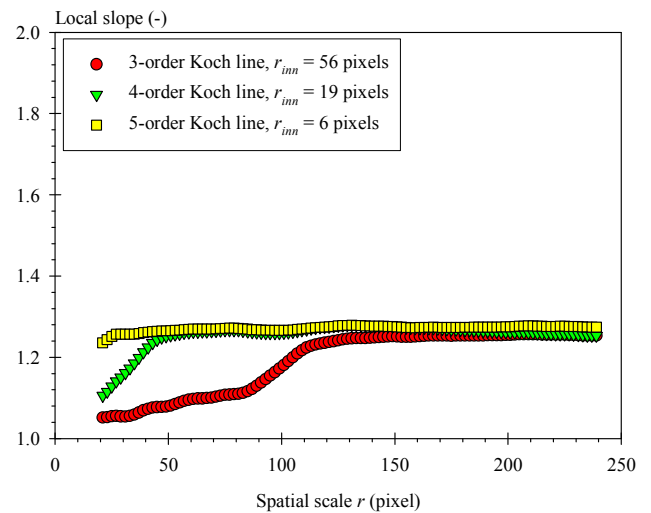


Figure 11: Influence of the inner cutoff scale on the local slope graph obtained with the EDM method.

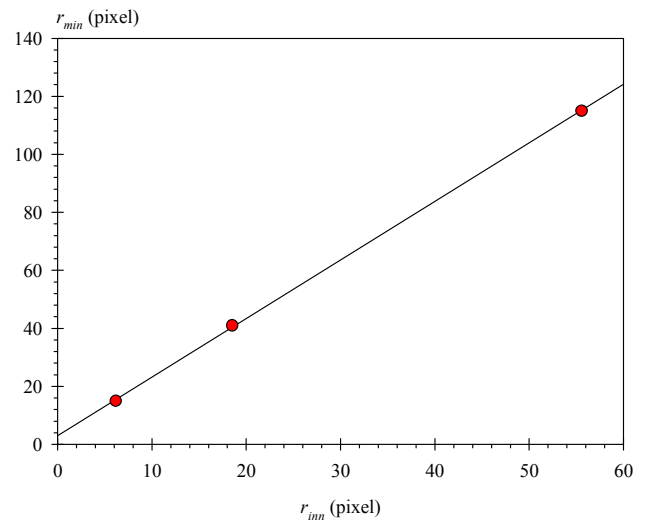


Figure 12: Comparison between the inner cutoff scale and the minimum spatial scale reported by the EDM method.

Finally, a last test on the propensity of the EDM method to determine the inner cutoff scale of a natural fractal is conducted. To achieve this, three series of Koch

line images of different order are analyzed. As the order of the Koch line varies, the inner cutoff scale, that is the smallest linear element constituting the line, varies also. In the present test, Koch lines of order 3, 4 and 5 are analyzed. Their respective inner cutoff scale is 56, 19 and 6 pixels. Each series is constituted of 200 images. The local slope graphs obtained for these three series are compared in Fig. 11. It can be first seen that for each series, the EDM method reports a spatial scale interval over which the objects are fractal with a fractal dimension equal to the expected value. Thus, the EDM method is very robust. Second, this figure shows that the minimum spatial scale r_{min} at which the local slope becomes constant increases with the inner cutoff scale of the object. Furthermore, the comparison between the scale r_{min} , calculated as being the spatial scale at which the local slope is equal to 98% of the measured fractal dimension, and the inner cutoff scale r_{inn} , reveals that these two scales are linearly related (see Fig. 12). Thus, the EDM method allows determining a spatial scale that is representative of the inner cutoff scale of the object, provided, of course, that this scale is within the resolved scale interval.

5. CONCLUSION

The analysis of sets of synthetic images with several fractal analysis methods presented in this paper leads to the following conclusions. Among the three methods tested, the EDM method is the best adapted. It allows determining the fractal dimension with a good accuracy. Furthermore it succeeds in describing the texture and the structure of an object and reports two fractal dimensions. One characterizes the tortuosity of the boundary of the object and the second one gives information on the shape of the whole object. It is believed that these two fractal dimensions can bring precious information on the organization of the liquid flow during the primary atomization process.

Another interesting aspect of the EDM method is that it is possible to apply it on a single image. Therefore, for given working conditions, it will be possible to determine the fractal dimension temporal distribution and to qualify the fractalness of the atomization process.

Finally, it has been shown that the EDM method allows also determining some representative spatial scales, such as a scale proportional to the inner cutoff scale of the object as well as the spatial scale delimiting the textural to the structural spatial scale interval.

One must insist on the fact that all these results are meaningful for the kind of images used in the present work only and that very different conclusions would be drawn for images of a different type.

6. NOMENCLATURE

K	constant [-]
$N(r)$	Number [-]
r	Spatial length scale [pixel]
r_{inn}	Lower cutoff scale [pixel]
r_{min}	Minimum spatial scale [pixel]
r_{out}	Upper cutoff scale [pixel]
δ	Fractal dimension [-]
ΔP_i	Injection pressure [Pa]

7. REFERENCES

- Chigier, N., The Future of Atomization and Sprays, Proc. 20th Annual Conference on Liquid Atomization and Sprays Systems – Europe, Orléans, France, 2005
- Dumouchel, C., Experimental Analysis of a Liquid Atomization Process at Low Weber Number, Int. Symp. Heat and Mass Transfers in Spray Systems, Antalya, Turkey, 2005
- Panico, J. and Sterling, P., Retinal Neurons and Vessels Are Not Fractal But Space-Filling, The Journal of Comparative Neurology, Vol. 361, pp. 479-490, 1995
- Caserta, F., Eldred, W.D., Fernandez, E., Hausman, R.E., Stanford, L.R., Bulderev, S.V., Schwarzer, S. and Stanley, H.E., Determination of Fractal Dimension of Physiologically Characterized Neurons in Two and Three Dimensions. Journ. Neuroscience Meth., Vol. 56, pp. 133-144, 1995
- Smith, T.G., Lange, G.D. and Marks, W.B., Fractal Methods and Results in Cellular Morphology – Dimensions, Lacunarity and Multifractals, Journ. Neuroscience Meth., Vol. 69, pp. 123-136, 1996
- Sreenivasan, K.R., Fractal and Multifractal in Fluid Turbulence. Annu. Rev. Fluid Mech., Vol. 23, pp. 539-600, 1991
- Hall, M.J., Dai, W. and Matthews, R.D., Fractal Analysis of Turbulent Premixed Flame Images from SI Engines, SAE Technical Paper n°92242, pp. 1931-1946, 1992
- Kaye, B.H., A Random Walk Through Fractal Dimensions, VCH, New-York, 1989
- Chehroudi, B. and Talley, D., The Fractal Geometry of Round Turbulent Cryogenic Nitrogen Jets at Subcritical and Supercritical Pressures, Atomization and Sprays, Vol. 14, pp. 81-91, 2004
- Shavit, U. and Chigier, N., Fractal Dimensions of Liquid Jet Interface Under Break-up, Atomization and Sprays, Vol. 5, pp. 525-543, 1995
- Dumouchel, C., Cousin, J. and Triballier, K., Experimental Analysis of Liquid-Gas Interface at Low Weber Number: Interface Length and Fractal Dimension, Exp. Fluids, Vol. 39, pp. 651-666, 2005
- Foroutan-pour, K., Dutilleul, P. and Smith, D.L., Advances in the Implementation of the Box-counting Method of Fractal Dimension Estimation, Applied Mathematics and Computation, Vol. 105, pp. 195-210, 1999
- Bérubé, D. and Jébrak, M., High Precision Boundary Fractal Analysis for Shape Characterization, Computers & Geosciences, Vol. 25, pp. 1059-1071, 1999
- Dumouchel, C., Cousin, J. and Triballier, K., On the Role of the Liquid Flow Characteristics on Low-Weber-Number Atomization Processes, Exp. Fluids, Vol. 38, pp. 637-647, 2005
- Triballier, K., Etude énergétique des processus d'atomisation primaire : Application au comportement des injecteurs essence basse pression à triple disque, Ph.D. thesis, Université de Rouen, 2003